THE EUROPEAN SOCIETY OF MEDICINE
Medical Research Archives, Volume 13 Issue 7

RESEARCH ARTICLE

Lack of HB-EGF Expression is Protective against Chronic Kidney Disease under Diabetic Conditions

Taylor SR[1], Duan E[1], Zhou Z[1], Harding PA[1]

[1] Department of Biology, Cell, Molecular Structural Biology Program, Miami University, Oxford, OH 45056, United States

OPEN ACCESS

PUBLISHED
30 June 2025

CITATION
Taylor, SR., Duan, E., et al., 2025. Lack of HB-EGF Expression is Protective against Chronic Kidney Disease under Diabetic Conditions. Medical Research Archives, [online] 13(7). https://doi.org/10.18103/mra.v13i7.6710

DOI
https://doi.org/10.18103/mra.v13i7.6710

ISSN
2375-1924

.

ABSTRACT

Chronic kidney disease affects about 1 out of 3 adults with diabetes that may result in kidney failure and possibly end-stage renal disease. The aim of this study is to determine the role of HB-EGF as a contributing factor to chronic kidney disease in streptozotocin induced diabetic mice. We find that streptozotocin-induced diabetic wild-type, human HB-EGF transgenic, HB-EGF heterozygous, and HB-EGF null mice resulted in hyperglycemic conditions compared to control mice, exhibited enlarged kidney size, weight, and glomerular cross-sectional area and were directly correlated to the levels of HB-EGF. Collagen formation was was observed in the kidneys of wild type, heterozygous, and transgenic streptozotocin-mice but absent in HB-EGF -/- as well as control mice suggesting that HB-EGF stimulates fibrosis. Serum insulin like growth factor-1 and insulin like growth factor binding protein-3 levels in streptozotocin-diabetic HB-EGF transgenic were significantly higher indicating HB-EGF may be contributing to chronic kidney disease. Collectively, these findings suggest that the lack of HB-EGF may be protective against steptozotocin-induced chronic kidney disease.

Keywords: HB-EGF, transgenic, streptozotocin, diabetic kidney disease

Introduction

Heparin-Binding EGF-like growth factor (HB-EGF) exhibits significant biological functions in both normal and pathological processes, including, but not limited to, wound healing, cell division, adipogenesis and fibrosis[1]. The role of growth factors in diabetes and renal injury is not fully understood, but the kidney has the ability to recover from injury, in part, by the action of HB-EGF[2]. The significance of this research provides a better understanding of the possible *in vivo* role(s) of HB-EGF and IGF-1/IGFBP-3 in DKD.

HB-EGF is a member of the EGF superfamily of proteins that are initially synthesized as single, type I, transmembrane precursor molecules that undergo extensive proteolytic processing resulting in the release of extracellular soluble, mature domain that binds to and stimulates EGF receptors which then ligand with EGF receptors (EGFRs) on the cell membrane[3]. EGF family members undergo ectodomain proteolytic processing by furin, tumor necrosis factor alpha-converting enzyme (TACE), a disintegrin and metalloproteases (ADAMs), and unknown transmembrane/intracellular domain enzyme(s) that further processes the intracellular domain.

HB-EGF binds to EGF receptors (EGFR) or HER1 as well as HER4, and activates the intrinsic receptor tyrosine kinase of these receptors[4]. HER1 and HER4 are both expressed in the kidney and involved in cellular growth, proliferation and differentiation[5]. Under normal conditions, HB-EGF is expressed at low levels in the kidney[6], however, in response to diabetes and acute renal injury HB-EGF mRNA is significantly upregulated in the distal tubules of the kidney[7-9] and the levels of HB-EGF protein increase. Since HB-EGF is a potent mitogen, it is hypothesized that HB-EGF may be responsible for renal regeneration and proliferation[3,10-13]. Consequently, upon the onset of diabetes and the subsequent rise of HB-EGF levels, renal hypertrophy occurs. Renal hypertrophy is a process that compensates for the loss of functioning renal tissue during injury and is considered an early manifestation of diabetes. Of particular note and relative to this study, albeit HB-EGF is expressed at low levels in the normal kidneys, it has been shown to be expressed in the glomerular mesangium of patients with glomerulonephritis[4]. Furthermore, IGFBP-3 has been shown to be downregulated in the kidney of HB-EGF transgenic mice, but recent studies demonstrate existence of anti-inflammatory action of IGFBP-3 in chronic kidney disease (CKD) reinforcing the concept in support of the clinical significance of the IGF-independent action of IGFBPs in the assessment of pathophysiology of kidney disease[14].

Diabetic nephropathy is a result of microvascular damage to the kidney. The basic functional unit of the kidney is the nephron composed of a glomerulus and renal tubules. The glomerulus is an arteriole globule surrounded by a parietal layer of Bowman's capsule. The different cell types in the capillary bed are glomerular podocytes, mesangial and endothelial cells, tubular epithelial cells, interstitial fibroblasts and vascular endothelial cells[15]. Glomerular podocytes are essential for the molecule size selectivity in the formation of primary urine. Massive podocytes cover the basal lamina around glomerular capillaries, leaving filtration slits among them. The slit diaphragms are covered by cell surface proteins and prevent large molecules and/or negatively charged proteins into primary urine from the bloodstream. Some important smaller molecules such as water and glucose in the primary urine are further reabsorbed by tubules of nephrons in the formation of urine. Additionally, intraglomerular mesangial cells are differentiated smooth muscle cells from pericytes, and located among the glomerular capillaries within renal corpuscles of a kidney. They function in regulating blood flow by contraction of glomerular capillaries in the basement membrane resulting in the restriction of filtration. The phagocytic nature of mesangial cells removes extra proteins and debris from capillary basement membrane. In addition, mesangial cells have the ability to secrete extracellular matrix proteins, prostaglandins, and cytokines.

Diabetic renal disease is characterized by sequential pathophysiologic changes, including glomerular and tubular hypertrophy, high glomerular filtration rate, microalbuminuria, extracellular matrix accumulation, renal fibrosis and renal failure. The mechanisms of these pathological events are in the cellular and extracellular damages in the glomerular and tubulo-interstitial compartments and are in part contributed to by HB-EGF[16]. Results presented in this study suggest that the lack of HB-EGF is protective against DKD.

Materials and Methods

ANIMALS

All protocols were approved by the Institutional Animal Care and Use Committee of Miami University. Ten-week human HB-EGF transgenic (TG) (FVB/N strain, n=24), HB-EGF null (129SVJ strain, n=24) (gift from Dr. Susan Wohler Sunnarborg, UNC-Lineberger Comprehensive Cancer Center), HB-EGF heterozygous (129SVJ strain, n=24), and wild-type 129SVJ mice, n=13 each), weighing approximately 20g were used in this study. Animals were housed as previously described[17]. Animals received daily injections for 5 consecutive days of STZ (300 mg/kg i.p.) freshly prepared in citrate buffer (0.05 M, pH 4.5). Additionally, HB-EGF transgenic, null, heterozygous, and wild-type strains were injected with citrate buffer (CB) only and serve as non-diabetic control mice for comparison. The onset of diabetes was determined by obtaining fasting blood glucose levels. Only animals with blood glucose levels 300 mg/dl or above were considered diabetic. Blood glucose was measured using a Bayer glucometer on blood samples after a 6 hour fast from the tail vein.

GENOTYPE DETERMINATION

The genotypes of mice were analyzed by the polymerase chain reaction (PCR) using total genomic DNA isolated from HB-EGF TG and null mice[17,18] from tail clips after proteinase K (1mg/ml) digestion and chloroform-isopropanol extraction. Human HB-EGF transgenic mice were genotyped using a human HB-EGF forward primer (5'-CGTCTGTAGCGACCCTTTGC-3'), and human HB-EGF reverse primer (5'-GTTCTGCTGGTAGTGGTCGGC GAGCTGCAC-3') and resulted in a 921bp human HB-EGF DNA product using the following parameters: 94°C (4 min) - 1 cycle, 94°C (30 sec), 57°C (30 sec), 72°C (1

min) - 35 cycles followed by 72°C extension for 10 min. Identification of the wild-type HB-EGF allele utilized a mouse HB-EGF wild type forward primer (5'-CTGACAGACCTTCAAGGGCT-3') and wild type reverse primer (5'-GCCAGACCTCTCCGAAGCCGC-3') and resulted in a 520bp genomic DNA product in wild type and heterozygous mice. HB-EGF null mice were analyzed using a mouse HB-EGF wild type forward primer and HB-EGF pSV-neo gene reverse primer and resulted in a 320bp DNA product. Wild-type and null genotypes utilized the following PCR parameters: 94°C (4 min) - 1 cycle, 94°C (30 sec), 58°C (30 sec), 72°C (45 sec) for 40 cycles followed by 72°C extension for 5 min.

KIDNEY ANALYSES

CB-treated non-diabetic and STZ-induced diabetic WT, null, HET, and HB-EGF TG mice were weighed, sacrificed, and both kidneys were collected. Kidneys were weighed and examined using an Olympus SZX12 microscope by camera (Nikon D300). Kidney weight to body weight ratios were determined and analyzed by an unpaired, two-tailed t-test and ANOVA.

Histopathological analyses of the kidneys from CB-treated non-diabetic and STZ-induced diabetic WT, null, HET, and HB-EGF TG mice (5 each) were fixed in 4 % paraformaldehyde/PBS for 24 hours at 4 °C, washed in PBS, and stored in 70% ethanol. Tissues were dehydrated, paraffin-embedded, sectioned (5 µm), and stained with hematoxylin-eosin (H&E). Additionally, kidney sections from CB-treated non-diabetic and STZ-induced diabetic WT, null, HET, and HB-EGF TG mice were examined for collagen expression using Masson's Trichrome stain according to manufacturer's recommendation (Sigma-Aldrich).

Following the detection of pathological damages in glomeruli and tubules, the area of glomeruli of CB-treated non-diabetic and STZ-induced diabetic WT, null, HET, and HB-EGF TG mice were determined from H&E-stained sections using an Olympus AX70 microscope (20× magnification). Images were acquired using a Nikon D300 camera. The area of each glomerulus was determined using Image Pro software. Thirty glomeruli of each mouse strain were measured and the average areas of CB-treated non-diabetic and STZ-induced diabetic WT, null, HET, and HB-EGF TG mice (3 each), were analyzed by student t-test and ANOVA.

COLLECTION OF SERUM PROTEINS

Whole blood was collected CB-treated non-diabetic and STZ-induced diabetic WT, null, HET, and HB-EGF TG mice and serum was isolated by centrifuging in a serum separator (BD Microtainer, NJ). Protein concentrations of serum were determined using BCA Protein Assay Kit (Pierce Biotechnology, Inc., Rockford, IL) following manufacturers suggestions.

IMMUNOBLOTTING ANALYSIS

250mg kidney tissue was sonicated in lysis buffer Protein concentrations were determined using BCA protein assay kit (Pierce) and total protein (10 ug) was separated by 12% sodium dodecyl sulfate polyacrylamide gel electrophoresis (SDS-PAGE) under reducing conditions, and transferred onto a PVDF membrane (Millipore). 0.1ug of recombinant human HB-EGF was used as a positive control. Membranes were blocked with Tris-buffered saline with Tween-20 (TBST) (0.1%Tween-20) plus 5% non-fat dry milk overnight at 4 C with gentle shaking, washed with TBST three times (15 min each), and probed with primary antibodies overnight at 4 C [rabbit anti C-terminus of human HB-EGF, 1:200; goat anti N-terminus of human HB-EGF, 1:200, R&D Systems (Minneapolis, MN); sheep anti-ADAM 12, 0.1mg/ml, R&D Systems], followed by incubation with HRP-conjugated secondary antibodies 1 h at room temperature (rabbit anti-goat IgG, or rabbit, Jackson ImmunoResearch Laboratories, West Grove, PA). Specific immunoreactivity was determined by application of SuperSignal West Pico Chemiluminescent Substrate (Pierce Biotechnology, Inc., Rockford, IL) to the membrane and normalized to actin[17].

IGFBP-3 protein levels were analyzed by western blot using 100 ug total serum proteins from CB-treated non-diabetic and STZ-induced diabetic WT, null, HET, and HB-EGF TG mice. Serum protein were separated by 12.5% non-reducing SDS polyacrylamide gel, transferred onto a PVDF membrane (Millipore: Billerica, MA) for 3 hours at 80 V at 4 °C in 1000 ml transfer buffer (3 g Tris, 14.4 g glycine, 5 ml 20 % SDS and 100 ml methanol), and blocked to prevent nonspecific antibody binding in 5% non-fat dry milk (NFDM) in 1×TBS buffer (0.8 % NaCl, 0.02 % KCl and 0.3 % Tris base, pH 7.4) with 1% Tween 20 (TBST) solution for 1 hour while rocking. The membranes were incubated with the primary antibody, a goat anti-mouse IGFBP-3 antibody (R&D Systems) at a concentration of 0.2 µg/ml in 5 % NFDM/TBST solution for 12 hours in 4°C while rocking. Membranes were then washed 3 times 10 minutes each in TBST solution at room temperature with gentle agitation to remove any unbound primary antibody. A horseradish peroxidase (HRP)-conjugated rabbit anti-goat IgG secondary antibody (R&D Systems) at a 1:10,000 dilution in 5 % NFDM/TBST solution was incubated on the blot for 2 hours at room temperature while rocking. After incubation the unbounded second antibody was removed from the membranes by washing 4 times 15 minutes each with TBST solution. Membranes were exposed to medical X-ray films (Fujifilm Corporation, Japan, Tokyo) using Supersignal West Pico Chemiluminescence detection system (Pierce Biotechnology, Inc.: Rockford, IL) per manufacturer's recommendations. The films were developed in the processor (Kodak, M35A X-OMAT). And after exposure and development, the films were scanned, and the digital images of scanned films were densitometric analyzed for quantitative data of immunoreactive IGFBP-3 protein from CB-treated non-diabetic and STZ-induced diabetic WT, null, HET, and HB-EGF TG mice. The pixel intensity of each individual band was determined as arbitrary optical density (AOD) by using Image Quant 5.2 software (Molecular Devices: Piscataway, NJ). After quantitative measurement, the data were analyzed by student t-test and ANOVA.

Upon the analysis of circulating IGFBP-3, the targeted protein IGF-I levels were also assessed by western blot. Seven hundred and fifty microgram total protein in serum of each mouse strain was loaded in a 12.5 % no reduction SDS PAGE. Following electrophoresis, the proteins were transferred onto a PVDF membrane

(Millipore: Billerica, MA) for 3.5 hours at 80 V at 4 °C. After transfer, the membrane was then blocked in a 5 % NFDM in TBST solution overnight. Following blocking, membranes were incubated with the primary antibody, a rabbit polyclonal to mouse IGF-I antibody (Abcam, Cambridge, MA) at a concentration of 2 µg/ml in 5 % NFDM/TBST solution for 12 hours at 4°C on shaking bed. Membranes were then washed 3 times 10 minutes each in TBST solution at room temperature with gentle agitation. An HRP-conjugated mouse anti-rabbit IgG secondary antibody (R&D Systems) at a 1:20,000 dilution in 5 % NFDM/TBST solution was incubated on the blot for 2 hours at room temperature and shaken gently. The membranes were washed 4 times 15 minutes each with TBST solution. And after exposure and development, the films were scanned, and the densitometric analysis of AOD of immunoreactive IGF-I protein from HB-EGF tg, heterozygous, null, and wild-type mice were determined by using ImageQuant 5.2 software (Molecular Devices: Piscataway, NJ). Similar to IGFBP-3, the quantitative data were analyzed by student t-test and ANOVA.

Gelsolin was used as internal control in serum for the circulating IGFBP-3 and IGF-I in the western blots. The total amount of 750 µg mouse serum proteins from CB-treated non-diabetic and STZ-induced diabetic WT, null, HET, and HB-EGF TG mice were loaded in a 12.5 % no reduction SDS polyacrylamide gel and electrophoresed at 100 V for 2 hours. After being separated in the gel, the proteins were transferred onto a PVDF membrane (Millipore: Billerica, MA) for 5.5 hours at 80 V in 4 °C. The membrane was then blocked in a 5 % NFDM/TBST solution overnight. Following blocking, membranes were incubated with the primary antibody, a goat polyclonal to mouse Gelsolin antibody (Abcam, Cambridge, MA) at a concentration of 1 µg/ml in 5 % NFDM/TBST solution for 12 hours at 4 °C on shaking bed. Gently agitated, the membranes were then washed 3 times 10 minutes each in TBST solution at room temperature. An HRP-conjugated rabbit anti-mouse IgG secondary antibody (R&D Systems) at a 1:10,000 dilution in 5 % NFDM/TBST solution was incubated on the blot for 2 hours at room temperature and shaken gently. The membranes were washed 4 times 15 minutes each with TBST solution. Proteins were visualized by the Membranes using the Supersignal West Pico Chemiluminescence detection system (Pierce Biotechnology, Inc.: Rockford, IL) and exposed to X-ray film. The quantitative data of immunoreactive Gelsolin protein from HB-EGF TG, heterozygous, null, and wild-type mice. The pixel intensity of each individual band was determined by using ImageQuant 5.2 software (Molecular Devices: Piscataway, NJ).

QUANTITATIVE PCR

Kidneys collected from CB-treated non-diabetic and STZ-induced diabetic WT, null, HET, and HB-EGF TG mice were frozen immediately in liquid nitrogen, homogenized by homogenizer (Powergen 700, Fisher Science) in TriReagent (Molecular Research Center, Cincinnati, OH). Total RNA was isolated from kidney homogenate after chloroform and isopropanol extraction, and dissolved in RNAse free water. The concentrations of RNA were measured by a NanoDrop machine.

In order to analyze the local effects of HB-EGF on IGFBP-3 in the kidney, 500 ng RNA was used as a template in semi-quantitative RT-PCR to detect renal IGFBP-3 mRNA level. The RT-PCR reactions were performed using a Superscript One-step RT-PCR kit (Invitrogen, Carlsbad, CA). The mouse IGFBP-3 forward primer is 5'-AGCCTAAGCACCTACCTCCC-3', and the reverse primer is 5'-CTC GGAGGAGAAGTTCTGGG-3' (243 bp). RT-PCR programs for IGFBP-3 were 50°C (30 minutes) for 1 cycle, 95°C (10 minutes) for 1 cycle, 95°C (30 seconds), 53°C (1 minute), 72°C (45 seconds) for 25 cycles, followed by an extension at 72°C for 10 minutes.

The glyceraldehyde-3-phosphate dehydrogenase (GAPDH) forward primer (5'-CCCTTCATTGACCTCAACT ACAT-3') and reverse primer (5'-ACAATGCCAAAGTTG TCATGG AT-3') were used as an internal control to assure integrity of the RNA samples. RT-PCR programs for GAPDH were 50°C (30 minutes) for 1 cycle, 94°C (30 seconds), 59°C (1 minute), 72 °C (45 seconds) for 30 cycles, followed by an extension at 72°C for 15 minutes. The PCR products were analyzed by agarose gel electrophoresis stained with ethidium bromide (EB).

QUANTITATIVE REAL TIME RT-PCR OF IGFBP-3 mRNA LEVEL DETECTION

In order to actually assess the mRNA expression of IGFBP-3 in kidneys of CB-treated non-diabetic and STZ-induced diabetic WT, null, HET, and HB-EGF TG mice, 200 ng template RNA was used in real time RT-PCR to detect accurate IGFBP-3 mRNA level in kidney. The real time RT-PCR reactions were performed using a Rotor gene 3000 RT-PCR machine (Corbett Life Science, AU). The mouse IGFBP-3 primers and GAPDH were described. RT-PCR programs for IGFBP-3 were 50°C (30 minutes) for 1 cycle, 94°C (5 minutes) for 1 cycle, 94°C (30 seconds), 50°C (30 seconds), 72°C (30 seconds) for 40 cycles, followed by an melt at 72°C to 99°C rising by 1°C each step, waiting for 45 seconds on first step and waiting for 5 seconds for each step afterwards.

Results

GENOTYPE DETERMINATION

In order to employ a mouse model that utilizes HB-EGF TG, heterozygous, null, and wild-type strains of mice, the polymerase chain reaction (PCR) was used to accurately genotype each mouse. The primers of human HB-EGF TG were used to amplify a 921 bp DNA product from HB-EGF TG mice. Genotyping HB-EGF null and heterozygous mice used a mouse HB-EGF wild type forward primer and a HB-EGF pSV-neo gene reverse primer and amplified a 320 bp DNA product in order to detect the null HB-EGF allele. The mouse HB-EGF wild type forward and reverse primers resulted in a 520 bp DNA product in wild type and heterozygous mice (Supplemental Fig. 1). Therefore, HB-EGF null mice are expected to result in a 320 bp DNA product only, HB-EGF wild type mice are expected to have a 520 bp DNA product only, while heterozygous mice are expected to have both 320 bp and 520 bp DNA products, and hHB-EGF TG mice are expected to have the 921bp transgene and an endogenous 320bp mHB-EGF product. Upon determining genotypes, the mice were housed under the same conditions with normal food, water, bedding, and light until 10 weeks old for use in this study.

STREPTOZOTOCIN (STZ)-INDUCED DIABETIC MICE

In order to determine the effects of HB-EGF on kidneys and on insulin signaling pathway, animals were made diabetic by daily intraperitoneal injection of STZ for 5 days in citrate buffer (CB) for HB-EGF TG, null, heterozygous, and wild-type strains, while the nondiabetic control mice were injected with CB only. Blood glucose levels were determined 24 hours after injection, and only animals with blood glucose levels 300 mg/dl or above were considered diabetic. Average blood glucose levels (n=50) over 3 weeks demonstrating STZ-induced hyperglycemia and normal blood glucose levels in citrate-buffer treated mice (Fig. 1A.). Blood glucose levels were determined each week thereafter until sacrificed. STZ-injected mice exhibited symptoms of being diabetic by exhibiting extremely wet bedding as compared to CB-nondiabetic mice suggestive of high urine output, characteristic of diabetes.

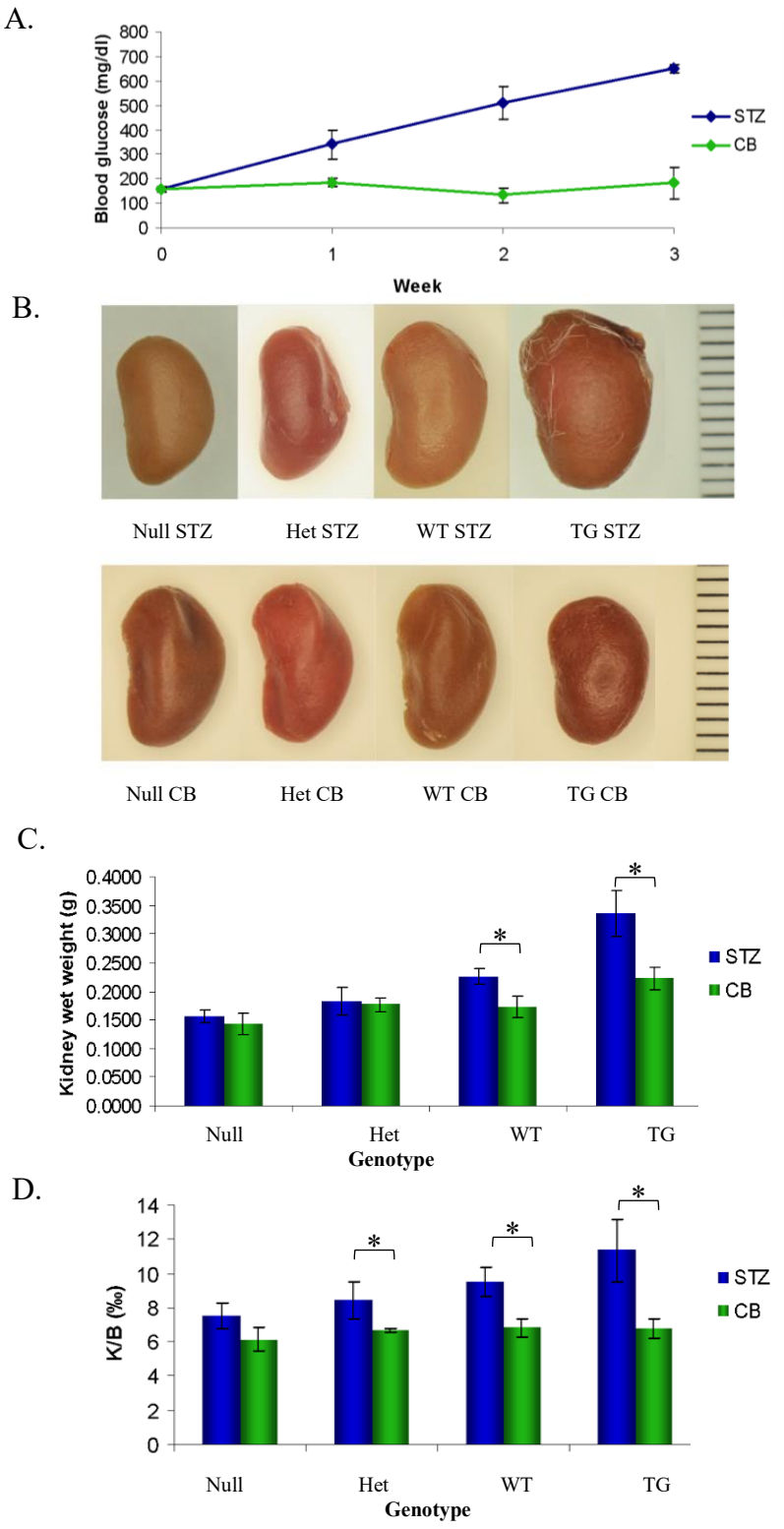

Figure 1. Analyses of kidneys from non-diabetic and diabetic null, heterozygous, wild-type, and HB-EGF transgenic mice. A. Mean blood glucose levels (mg/dl) of serum, **B.** Overt kidney measurement (mm), **C.** Wet weight of kidneys (g), and **D.** Kidney wet weight to body weight ratios (g) from streptozotocin (STZ) or citrate buffer (CB)-treated null, Het, WT, and TG mice (n=10 mice each). from STZ- and CB-treated null, Het, WT, and TG mice (n=10 each). Data were analyzed by student T-test and ANOVA (n=10 each), * $p<0.05$.

KIDNEY ANALYSIS

Upon successful generation of STZ-induced diabetic HB-EGF TG, heterozygous, null and wild type strains as well as non-diabetic control mice, animals were sacrificed at 13 weeks of age after 3 weeks exposure of STZ or CB. The general observation on the kidneys' size from WT, null, HET, and HB-EGF TG mice STZ-diabetic mice indicated that the higher levels of HB-EGF expression resulted in a larger kidney size (Figure 1.B.). Western blot analysis was performed on whole kidney protein extracts from WT (FVN/N and 129-SVJ), null, HET, and HB-EGF TG mice demonstrating HB-EGF immunoreactive proteins of 20 and 22kDa at the highest level in HB-EGF TG mice and lesser immunoreactivity in WT and HET mice, while no HB-EGF immunoreactive proteins were detected in the kidney of HB-EGF null mice. Recombinant HB-EGF was used as a positive control for HB-EGF immunoreactivity (Supplemental Fig. 2).

KIDNEY WET WEIGHT

The kidneys of STZ-induced diabetic HB-EGF TG and WT mice were significantly heavier than their CB-nondiabetic HB-EGF TG and WT control mice, but STZ-induced diabetic Het and null mice were not significantly heavier that the CB-nondiabetic Het and null control mice (Fig. 1. C). Because of the difference between the two strains of mice used in this study, the kidney wet weight of CB-nondiabetic HB-EGF TG mice in a FVB/N background were significantly higher compared to the CB-nondiabetic heterozygous, null, and wild-type mice of 129SVJ background, while no differences were observed between the CB-nondiabetic heterozygous, null, and wild-type mice (Fig. 1.C.). Kidney weights from 129SVJ WT strains of STZ-diabetic mice were significantly heavier than STZ-diabetic Het and null mice (Figure 1.C.). No statistical kidney weight differences were observed between STZ-diabetic HB-EGF Het and null mice compared to the CB-nondiabetic control mice (Fig. 1.C.). Values are the means ± SD. *p < 0.05 vs. control group.

KIDNEY/BODY WEIGHT RATIO

In order to account for the difference in mouse strains, the kidney weight to total body weight ratio (K/B) was analyzed. There was no difference in the kidney weight to bodyweight ratio (K/B) in either FVB/N or 129SVJ mouse strains with CB-nondiabetic mice. Significant differences were observed with K/B of STZ-induced diabetic WT, HET, and HB-EGF TG mice compared to CB-nondiabetic WT, HET, and HB-EGF TG control mice (Fig. 1.D.) No significant difference in K/B were observed in the HB-EGF null STZ-diabetic and CB-nondiabetic mice (Fig. 1.D.). Values are the means ± SD. *p < 0.05 vs. control group.

HISTOLOGICAL ANALYSES OF KIDNEY

H&E staining of kidneys from STZ-diabetic and CB-nondiabetic WT, null, HET, and HB-EGF TG mice was performed and demonstrated glomerular enlargement and renal cytotoxicity was observed in STZ-diabetic HB-EGF TG at the highest level and less in STZ-nondiabetic WT mice compared to CB-nondiabetic HB-EGF TG and WT control mice (Fig. 2.A.). No significant differences in glomerular enlargement were observed between STZ-diabetic null and HET mice and were similar to CB-nondiabetic control mice (Fig. 2.A). Furthermore, no differences in glomeruli were observed from CB-nondiabetic WT, null, HET, and HB-EGF TG mice (Fig. 2.A.).

A.

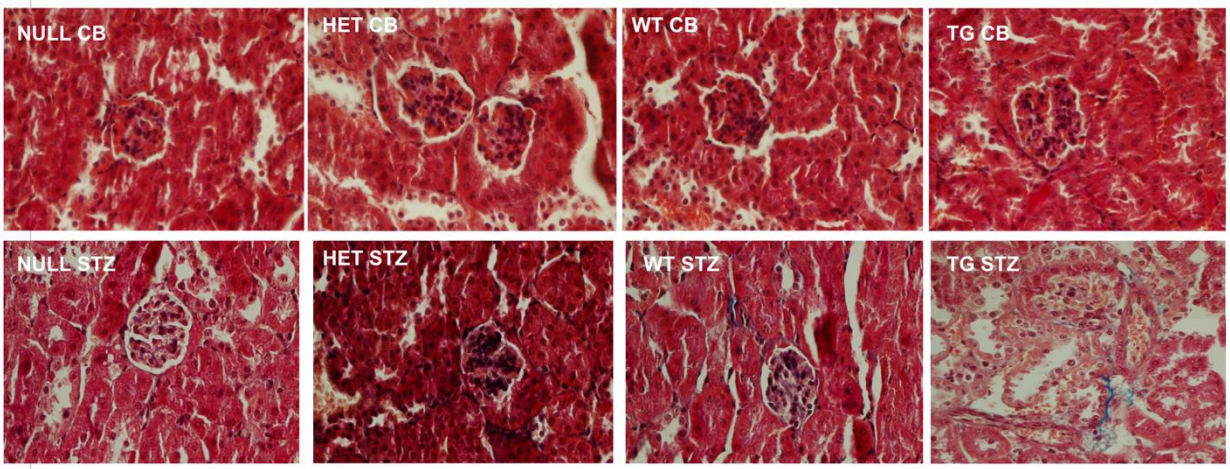

B.

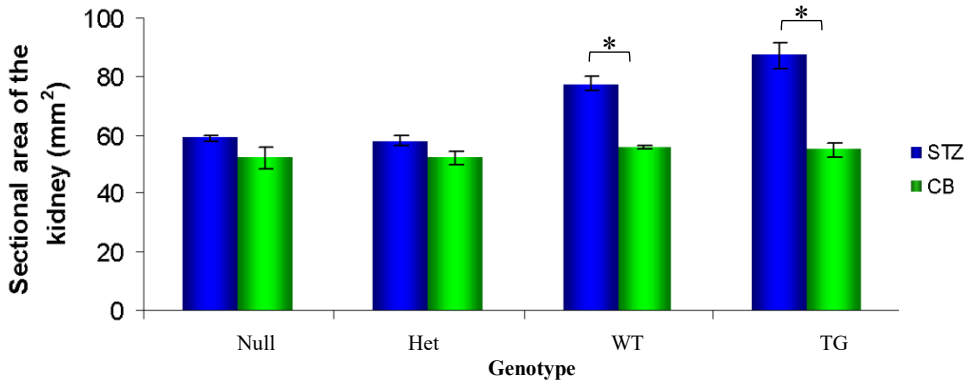

C.

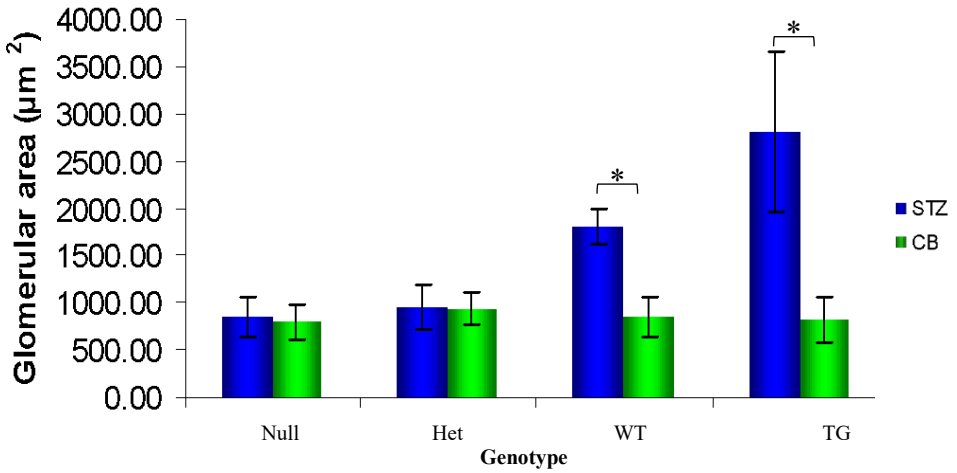

Figure 2. Cross-sectional of kidneys from non-diabetic and diabetic null, heterozygous, wild-type, and HB-EGF transgenic mice. A. H&E staining of individual glomeruli from kidneys (representation of 5 glomeruli of 5 different mice each), **B.** Total cross-sectional area of kidney, and **C.** Glomerular cross-sectional area from CB- and STZ-treated null, heterozygous, wild-type, and HB-EGF transgenic mice. Data were analyzed by Student's T-test and ANOVA (n=10 each), * $p< 0.05$.

Total kidney cross-sectional area of WT, null, HET, and HB-EGF TG STZ-diabetic and CB-nondiabetic mice from histological stained sections were examined and resulted in significantly increased kidney cross-sectional area in STZ-induced diabetic HB-EGF TG and WT mice compared to their CB-nondiabetic HB-EGF TG and WT control mice, whereas the kidney cross-sectional area of STZ-diabetic Het and null mice were not significantly different compared to CB-nondiabetic Het and null control mice (Fig. 2. B). Furthermore, the cross-sectional area of glomeruli from WT, null, HET, and HB-EGF TG STZ-diabetic and CB-nondiabetic mice were examined. Histological staining of kidney sections from STZ-induced diabetic HB-EGF TG and WT mice exhibited enlarged glomerular cross-sectional area compared to their CB-nondiabetic HB-EGF TG and WT control mice. The glomerular cross-sectional area of STZ-diabetic Het and null mice were not significantly different compared to CB-nondiabetic Het and null control mice (Fig. 2.C.). Values are the means ± SD. *p < 0.05 vs. control group.

MASSON'S TRICHROME

Renal hypertrophy is one of the early pathological damages due to diabetes and subsequent renal disease[19] and renal fibrosis is a development of renal nephropathy upon hypertrophy characterized by formation and deposition of excess extracellular matrix protein including fibrous connective tissues such as collagen and elastin that may be detected with Masson's trichrome staining. Masson trichrome staining was performed with STZ-diabetic and CB-nondiabetic WT, null, HET, and HB-EGF TG mice. Positive Masson's trichrome staining for collagen fibers (blue) were detected in the kidneys of STZ-diabetic HB-EGF TG and WT mice compared to CB-nondiabetic control HB-EGF TG and WT mice that lacked trichrome staining in the kidneys (Fig. 3.A.). Trichrome staining was detected neither in STZ-diabetic nor CB-nondiabetic HET and null mice (Fig.3.A).

A.

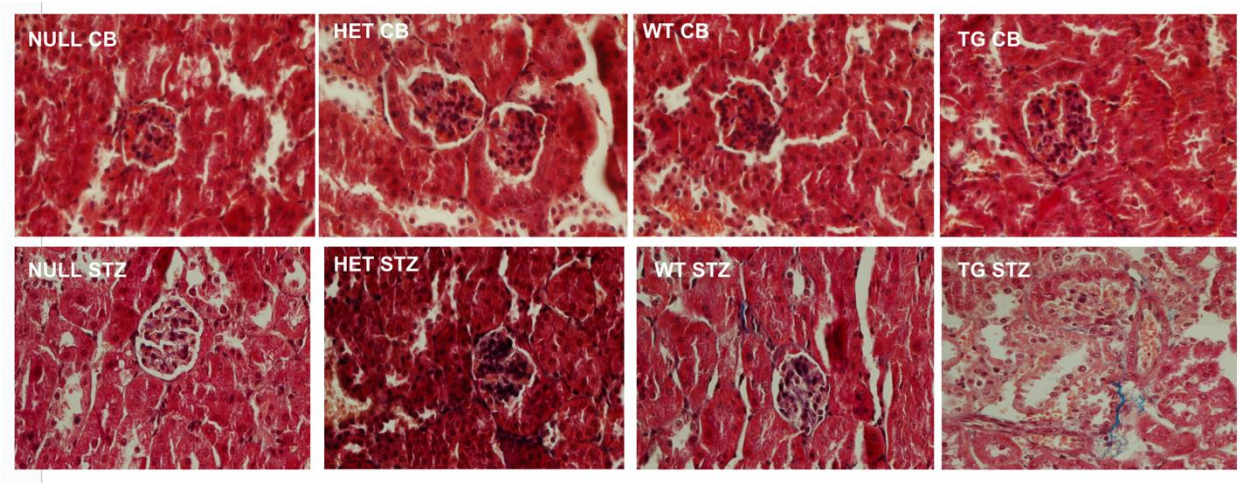

B.

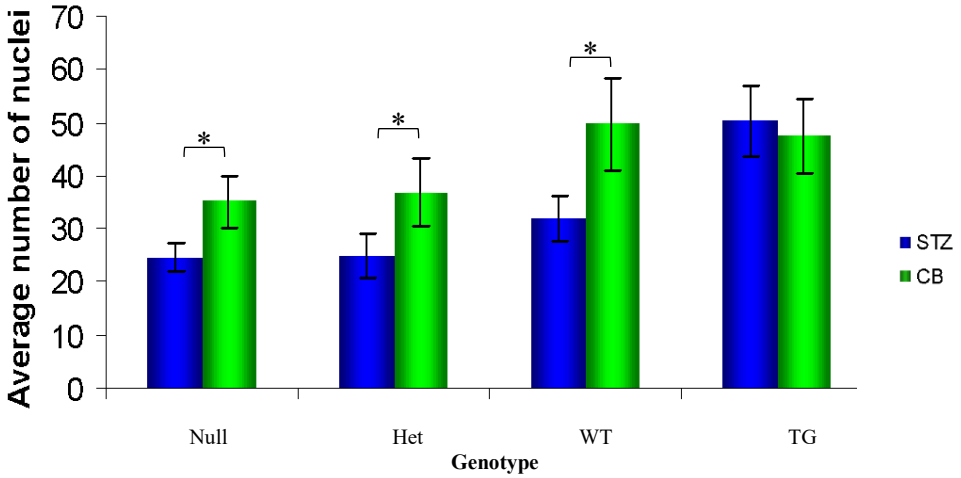

Figure 3. Glomerular analysis of non-diabetic and diabetic null, heterozygous, wild-type, and HB-EGF transgenic mice. A. Masson's trichrome staining of CB- and STZ-treated null, heterozygous, wild-type, and HB-EGF transgenic mice (representation of 5 glomeruli of 5 different mice each). **B.** Mean number of glomerular nuclei per glomeruli area from CB- and STZ-treated null, heterozygous, wild-type, and HB-EGF transgenic mice (representation of 5 glomeruli of 5 different mice each). Data were analyzed by Student's T-test. * $p < 0.05$.

STZ-induced diabetic WT, HET, and null mice exhibited a significant decrease in the total number of nuclei per glomeruli compared to CB-nondiabetic WT, HET, and null mice, but STZ-diabetic HB-EGF TG exhibited a significant increase in the total number of nuclei compared to CB-nondiabetic HB-EGF TG control mice. No differences were observed in the total number of glomerular nuclei in CB-nondiabetic WT, null, HET, and HB-EGF TG mice (Fig. 3.B.). Values are the means ± SD. *p < 0.05 vs. control group.

IGFBP-3 AND IGF-1 PROTEIN ANALYSES

Insulin-like growth factor-I (IGF-I) and insulin-like growth factor binding protein-3 (IGFBP-3) are both synthesized in the liver and delivered to target organs. Circulating IGF-I and IGFBP-3 from the serum of STZ-diabetic and CB-nondiabetic WT, null, HET, and HB-EGF TG mice were analyzed. STZ-diabetic HB-EGF TG mice demonstrated significantly higher levels of 45kDa IGFBP-3 compared to CB-nondiabetic mice (lanes 7 and 8, respectively) while STZ-diabetic WT (lane 1), null (lane 3), and HET IGFBP-3 (lane 5) levels were not significantly different compared to CB-nondiabetic WT, null, and HET IGFBP-3 levels (Fig. 4.A, lanes 2, 4, and 6, respectively; and D.). Gelsolin, an 82 kDa actin-depolymerizing protein expressed in serum, was used as an internal standard to quantitate the relative levels of expression of both IGFBP-3 and IGF-1[20] (Fig. 4.C.). Similarly, the serum IGF-1 levels in STZ-diabetic HB-EGF TG were significantly higher than the serum IGF-1 levels in CB-nondiabetic HB-EGF TG mice (Fig. 4.B, lanes 7 and 8, respectively) whereas STZ-diabetic and CB-nondiabetic serum IGF-1 levels in HET and WT mice were not significantly different (Fig. 4.B, lanes 3-6; and E.). However, the serum IGF-1 levels of STZ-diabetic null mice were significantly lower than the levels of CB-nondiabetic null mice (Fig. 4.B, lanes 1 and 2, respectively and E.). Values are the means ± SD. *p < 0.05 vs. control group.

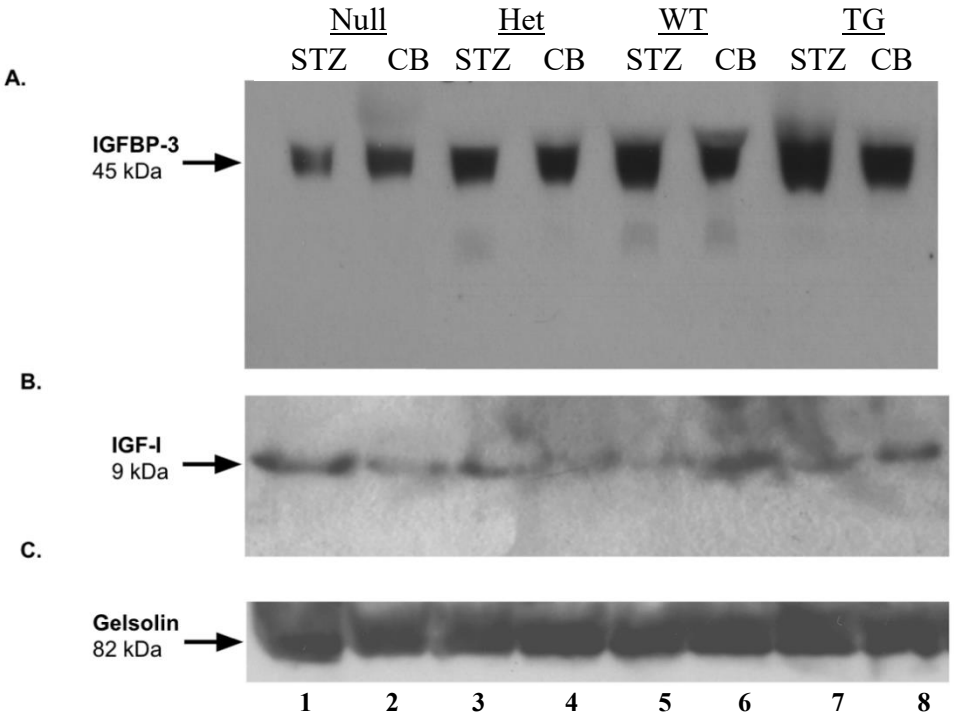

D.

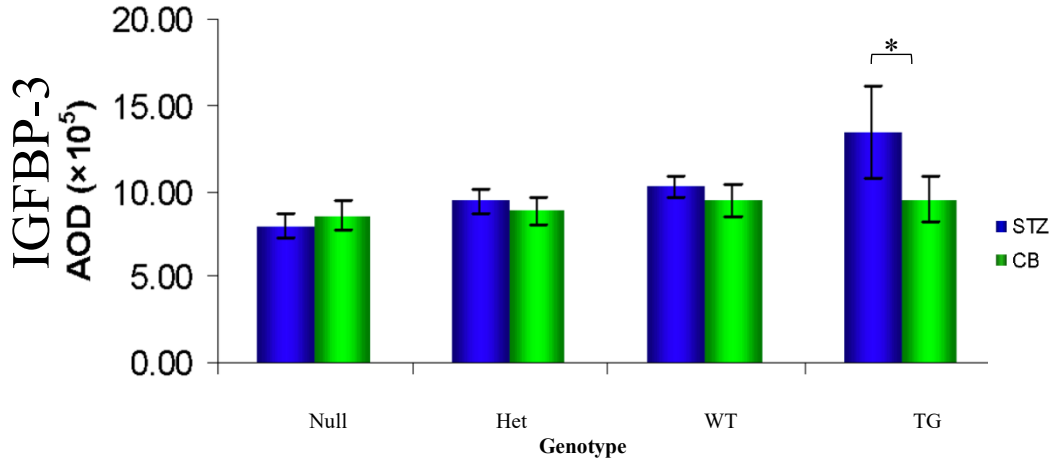

E.

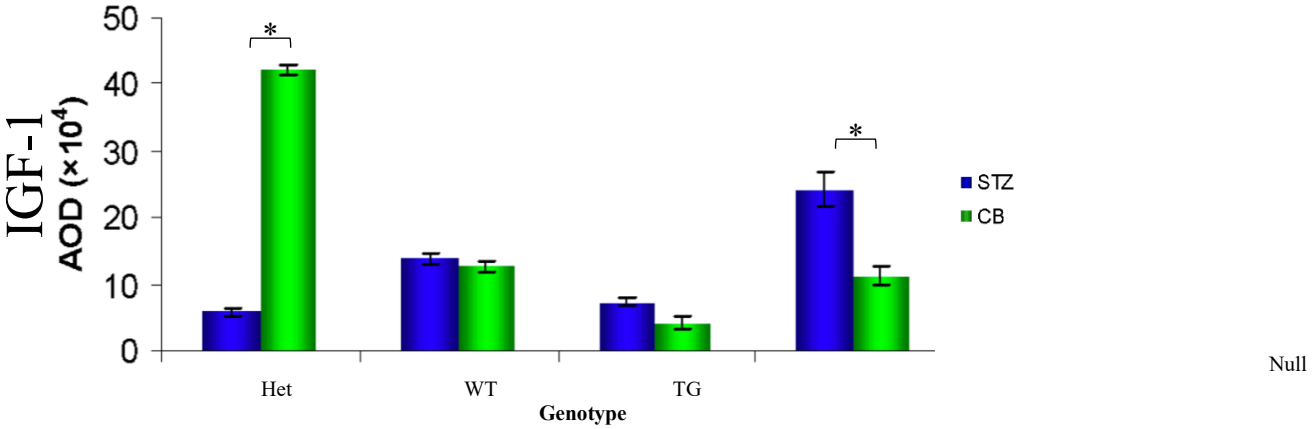

Figure 4. Insulin-like growth factor action in non-diabetic and diabetic null, heterozygous, wild-type, and HB-EGF transgenic mice. Western blot analysis of **A.** IGFBP-3 (45kDa), **B.** IGF-1 (9kDA), and **C.** gelsolin serum protein standard (82kDa) from kidneys of STZ- and CB-treated null (lanes 1,2), heterozygous (lanes 3,4), wild-type (lanes 5,6), and HB-EGF transgenic mice (lanes 7,8), respectively. Densitometric analysis of **D.** IGFBP-3 and **E.** IGF-1 protein levels compared to gelsolin proteins levels between CB- and STZ-treated null, heterozygous, wild-type, and HB-EGF transgenic mice. Data were analyzed by Student's T-test and ANOVA, * $p<0.05$.

Discussion

According to the American Diabetes Association, 23.6 people in the United States have diabetes, a disease characterized by the inability of the body to either synthesize or utilize insulin, and is the leading cause of kidney failure. According to the World Health Organization, about 422 million people worldwide have diabetes, and 1.5 million deaths are directly attributed to diabetes each year. Recent studies have provided evidence indicating the importance of EGFRs in the development of renal fibrosis in response to kidney injury[5] and reduced urinary EGF has been associated with chronic kidney disease[20], but the role of EGF/EGFR contributing to CKD is unclear. In the current study, we examine an EGFR ligand, HB-EGF, and its expression levels contributing to diabetic kidney disease *in vivo*.

Diabetes has been a focus of intense research for over 30 years, but little has been done to investigate the role of growth factors in diabetes, until recently. The kidney has the ability to recover from injury, in part, by the aid of HB-EGF, which was initially identified in the conditioned medium of human macrophages as a growth factor that binds to heparin and is mitogenic in epithelial cells, smooth muscle cells, but not endothelial cells[10,22]. In humans, HB-EGF is normally expressed in the lung, heart, brain, and skeletal muscle[6] and plays a large role in cellular proliferation[3,10-13,23,24] and heart development [18,25]. HB-EGF belongs to the epidermal growth factor (EGF) family which binds to and activates EGF receptors (EGFR)[10]. HB-EGF is initially synthesized as a type I transmembrane precursor protein (proHB-EGF) composed of a signal peptide, heparin-binding, EGF-like, juxtamembrane, transmembrane, and cytoplasmic domains[26]. It is well established that newly synthesized proHB-EGF undergoes amino-terminal processing at Arg[62]-Asp[63] by the endoprotease furin[27], followed by proteolytic cleavage at Pro[149]-Val[150] by "a disintegrin and metalloprotease" (ADAM) resulting in the release of a soluble form of HB-EGF, collectively referred to as "ectodomain shedding" [28,29] and can be induced by phorbol esters, 12-O-tetracanoylphorbol-13-acetate, TPA, phorbol 12-myristate 13-acetate (PMA)[3,30,31]. Subsequent to and dependent upon generation of soluble HB-EGF by ADAM cleavage, a carboxy-terminal region is generated, termed HB-EGF-C[29]. Both soluble, mature

HB-EGF and HB-EGF C are each capable of stimulating cellular division in EGFR-dependent and EGFR-independent pathways, respectively[29].

Under normal conditions, HB-EGF is expressed at low levels in the kidney[6]; however, in response to diabetes and acute renal injury, HB-EGF mRNA is significantly upregulated in the distal tubules of the kidney[7-9] and the levels of HB-EGF protein increase. The mitogen, HB-EGF, is likely responsible for renal regeneration and proliferation [3,10,11,13]. Consequently, after the onset of diabetes and the subsequent rise of HB-EGF protein levels, renal hypertrophy occurs. Renal hypertrophy is a process that compensates for the loss of functioning renal tissue during injury and is considered an early manifestation of diabetes. Data presented in this study indicates that increasing levels of HB-EGF potentiate renal glomerular hypertrophy and fibrosis, as demonstrated using STZ-induced diabetic HB-EGF transgenic mice that express the highest levels in the kidney and to a lesser extent in wild-type diabetic mice. HB-EGF heterozygous and null mice exhibited no noticeable renal disorders. Therefore, we conclude that the lack of HB-EGF expression in the kidney under STZ-induced diabetic conditions appears to be protective against renal nephropathy.

Furthermore, the insulin-like growth factor (IGF) – insulin-like growth factor binding protein (IGFBP) axis plays a critical role in the maintenance of normal renal function and the pathogenesis CKD. Serum IGF-I and IGFBPs are altered with different stages of CKD, the speed of onset, the amount of proteinuria, and the potential of remission. The role of IGF-I within the kidney is not completely understood, but has been shown to affect kidney growth, structure, and function[32-34]. Relative to the findings presented in this study, overexpression of IGF-I in TG mice likely induced renal and glomerular hypertrophy[35-37], which reflects the pathology observed in STZ TG mice that exhibited elevated levels of serum IGF-1 protein. Interestingly, STZ-treated HB-EGF null mice demonstrated significantly lower serum IGF-I levels compared to control mice, suggesting that IGF-I may play a significant role in CKD in diabetic conditions that is absent in HB-EGF null mice. In contrast STZ-treated HB-EGF TG demonstrated elevated levels of IGF-1 that may likely be attempting to respond to renal injury.

In patients with CKD, serum IGF-I levels are generally low along with elevated serum IGFBP-3 levels because of an increase of immunoreactive IGFBP-3 fragments, which exhibit reduced IGF-I affinity, whereas intact IGFBP-3 levels are not elevated. However, our results suggest intact IGFBP-3 of approximately 45kDa whereas the expected size of IGFBP-3 upon proteolysis would be a MW of 30kDa. The elevated serum IGF-I / IGFBP-3 axes, as a result of HB-EGF expression, is somewhat unexpected. However, it has been shown that the administration of IGF-1 improves renal function after acute renal failure[38] and in chronic renal failure (CRF)[39,40]. IGF-I administration results in an improvement in renal function and an increase in kidney size over 4 days in patients with advanced CRF[41]. The elevated serum IGF-1 in our HB-EGF STZ TG mice may be attempting to improve renal function as well as contributing to the overall increase in kidney size in diabetic mice, but may not be enough to overcome CKD, while the lack of HB-EGF expression lacks detectable CKD.

Conclusion:

The current study demonstrates that HB-EGF is likely a contributing factor to progression of CKD that results in enlarged kidneys and glomeruli, including collagen formation in diabetic mice, but mice that lack HB-EGF expression are protective against CKD. This study also suggests that HB-EGF may contribute to CKD through increased levels of IGFBP-3 and IGF-1 proteins, whereas diabetic null, heterozygous, and wild-type mice that exhibit indistinguishable levels result in little to no CKD. In summary, the severity of CKD correlates to the levels of expression of HB-EGF in diabetic mice.

References:

1. Taylor SR, Markesbery MG, Harding PA. Heparin-binding epidermal growth factor-like growth factor (HB-EGF) and proteolytic processing by a disintegrin and metalloproteinases (ADAM): a regulator of several pathways. *Semin Cell Dev Biol*. 2014;28:22-30. doi:10.1016/j.semcdb.2014.03.004
2. Daher A, de Boer WI, El-Marjou A, et al. Epidermal growth factor receptor regulates normal urothelial regeneration. *Lab Invest*. 2003;83(9):1333-1341. doi:10.1097/01.lab.0000086380.23263.52
3. Raab G, Klagsbrun M. Heparin-binding EGF-like growth factor. *Biochim Biophys Acta*. 1997;1333(3):F179-F199. doi:10.1016/s0304-419x(97)00024-3
4. Melenhorst WB, Mulder GM, Xi Q, et al. Epidermal growth factor receptor signaling in the kidney: key roles in physiology and disease. *Hypertension*. 2008;52(6):987-993. doi:10.1161/HYPERTENSIONAHA.108.113860
5. Cao S, Pan Y, Terker AS, et al. Epidermal growth factor receptor activation is essential for kidney fibrosis development. *Nat Commun*. 2023;14(1):7357. Published 2023 Nov 14. doi:10.1038/s41467-023-43226-x
6. Abraham JA, Damm D, Bajardi A, Miller J, Klagsbrun M, Ezekowitz RA. Heparin-binding EGF-like growth factor: characterization of rat and mouse cDNA clones, protein domain conservation across species, and transcript expression in tissues. *Biochem Biophys Res Commun*. 1993;190(1):125-133. doi:10.1006/bbrc.1993.1020
7. Lee YJ, Shin SJ, Lin SR, Tan MS, Tsai JH. Increased expression of heparin binding epidermal growth-factor-like growth factor mRNA in the kidney of streptozotocin-induced diabetic rats. *Biochem Biophys Res Commun*. 1995;207(1):216-222. doi:10.1006/bbrc.1995.1175
8. Homma T, Sakai M, Cheng HF, Yasuda T, Coffey RJ Jr, Harris RC. Induction of heparin-binding epidermal growth factor-like growth factor mRNA in rat kidney after acute injury. *J Clin Invest*. 1995;96(2):1018-1025. doi:10.1172/JCI118087
9. Sakai M, Zhang M, Homma T, et al. Production of heparin binding epidermal growth factor-like growth factor in the early phase of regeneration after acute renal injury. Isolation and localization of bioactive molecules. *J Clin Invest*. 1997;99(9):2128-2138. doi:10.1172/JCI119386
10. Higashiyama S, Abraham JA, Miller J, Fiddes JC, Klagsbrun M. A heparin-binding growth factor secreted by macrophage-like cells that is related to EGF. *Science*. 1991;251(4996):936-939. doi:10.1126/science.1840698
11. Higashiyama S, Lau K, Besner GE, Abraham JA, Klagsbrun M. Structure of heparin-binding EGF-like growth factor. Multiple forms, primary structure, and glycosylation of the mature protein. *J Biol Chem*. 1992;267(9):6205-6212.
12. Higashiyama S, Abraham JA, Klagsbrun M. Heparin-binding EGF-like growth factor stimulation of smooth muscle cell migration: dependence on interactions with cell surface heparan sulfate. *J Cell Biol*. 1993;122(4):933-940. doi:10.1083/jcb.122.4.933
13. Ito N, Kawata S, Tamura S, et al. Heparin-binding EGF-like growth factor is a potent mitogen for rat hepatocytes [published correction appears in Biochem Biophys Res Commun 1994 Mar 15;199(2):1088]. *Biochem Biophys Res Commun*. 1994;198(1):25-31. doi:10.1006/bbrc.1994.1004
14. Oh Y. The insulin-like growth factor system in chronic kidney disease: Pathophysiology and therapeutic opportunities. *Kidney Res Clin Pract*. 2012;31(1):26-37. doi:10.1016/j.krcp.2011.12.005
15. Kanwar YS, Wada J, Sun L, et al. Diabetic nephropathy: mechanisms of renal disease progression. *Exp Biol Med (Maywood)*. 2008;233(1):4-11. doi:10.3181/0705-MR-134
16. Reddy AS. (2004) Diabetic nephropathy: theory & practice. East Hanover.
17. Provenzano AP, Besner GE, James PF, Harding PA. Heparin-binding EGF-like growth factor (HB-EGF) overexpression in transgenic mice downregulates insulin-like growth factor binding protein (IGFBP)-3 and -4 mRNA. *Growth Factors*. 2005;23(1):19-31. doi:10.1080/08977140512331344012
18. Jackson LF, Qiu TH, Sunnarborg SW, et al. Defective valvulogenesis in HB-EGF and TACE-null mice is associated with aberrant BMP signaling. *EMBO J*. 2003;22(11):2704-2716. doi:10.1093/emboj/cdg264
19. Zerbini G, Gabellini D, Maestroni S, Maestroni A. Early renal dysfunctions in type 1 diabetes and pathogenesis of diabetic nephropathy. *J Nephrol*. 2007;20 Suppl 12:S19-S22.
20. Colquhoun DR, Goldman LR, Cole RN, et al. Global screening of human cord blood proteomes for biomarkers of toxic exposure and effect. *Environ Health Perspect*. 2009;117(5):832-838. doi:10.1289/ehp.11816
21. Zeid AM, Lamontagne JO, Zhang H, Marneros AG. Epidermal growth factor deficiency predisposes to progressive renal disease. *FASEB J*. 2022;36(5):e22286. doi:10.1096/fj.202101837R
22. Besner G, Higashiyama S, Klagsbrun M. Isolation and characterization of a macrophage-derived heparin-binding growth factor. *Cell Regul*. 1990;1(11):811-819. doi:10.1091/mbc.1.11.811
23. Kiso S, Kawata S, Tamura S, et al. Liver regeneration in heparin-binding EGF-like growth factor transgenic mice after partial hepatectomy. *Gastroenterology*. 2003;124(3):701-707. doi:10.1053/gast.2003.50097
24. Means AL, Ray KC, Singh AB, et al. Overexpression of heparin-binding EGF-like growth factor in mouse pancreas results in fibrosis and epithelial metaplasia. *Gastroenterology*. 2003;124(4):1020-1036. doi:10.1053/gast.2003.50150
25. Iwamoto R, Yamazaki S, Asakura M, et al. Heparin-binding EGF-like growth factor and ErbB signaling is essential for heart function. *Proc Natl Acad Sci U S A*. 2003;100(6):3221-3226. doi:10.1073/pnas.0537588100
26. Naglich JG, Metherall JE, Russell DW, Eidels L. Expression cloning of a diphtheria toxin receptor: identity with a heparin-binding EGF-like growth

factor precursor. *Cell*. 1992;69(6):1051-1061. doi:10.1016/0092-8674(92)90623-k

27. Nakagawa T, Higashiyama S, Mitamura T, Mekada E, Taniguchi N. Amino-terminal processing of cell surface heparin-binding epidermal growth factor-like growth factor up-regulates its juxtacrine but not its paracrine growth factor activity. *J Biol Chem*. 1996;271(48):30858-30863. doi:10.1074/jbc.271.48.30858
28. Asakura M, Kitakaze M, Takashima S, et al. Cardiac hypertrophy is inhibited by antagonism of ADAM12 processing of HB-EGF: metalloproteinase inhibitors as a new therapy. *Nat Med*. 2002;8(1):35-40. doi:10.1038/nm0102-35
29. Nanba D, Toki F, Higashiyama S. Roles of charged amino acid residues in the cytoplasmic domain of proHB-EGF. *Biochem Biophys Res Commun*. 2004;320(2):376-382. doi:10.1016/j.bbrc.2004.05.176
30. Goishi K, Higashiyama S, Klagsbrun M, et al. Phorbol ester induces the rapid processing of cell surface heparin-binding EGF-like growth factor: conversion from juxtacrine to paracrine growth factor activity. *Mol Biol Cell*. 1995;6(8):967-980. doi:10.1091/mbc.6.8.967
31. Gechtman Z, Alonso JL, Raab G, Ingber DE, Klagsbrun M. The shedding of membrane-anchored heparin-binding epidermal-like growth factor is regulated by the Raf/mitogen-activated protein kinase cascade and by cell adhesion and spreading. *J Biol Chem*. 1999;274(40):28828-28835. doi:10.1074/jbc.274.40.28828
32. Schaefer F and Rabkin R (2003) Insulin-like growth factor and the kidney. In: LeRoith D., Zumkeller W., Baxter R.C., editors. Insulin-like Growth Factors. Kluwer Academic/Plenum Publishers; New York: 2003. pp. 244–255.
33. Roelfsema V, Clark RG. The growth hormone and insulin-like growth factor axis: its manipulation for the benefit of growth disorders in renal failure. *J Am Soc Nephrol*. 2001;12(6):1297-1306. doi:10.1681/ASN.V1261297
34. Hirschberg R, Adler S. Insulin-like growth factor system and the kidney: physiology, pathophysiology, and therapeutic implications. *Am J Kidney Dis*. 1998;31(6):901-919. doi:10.1053/ajkd.1998.v31.pm9631833
35. Mathews LS, Hammer RE, Behringer RR, et al. Growth enhancement of transgenic mice expressing human insulin-like growth factor I. *Endocrinology*. 1988;123(6):2827-2833. doi:10.1210/endo-123-6-2827
36. Quaife CJ, Mathews LS, Pinkert CA, Hammer RE, Brinster RL, Palmiter RD. Histopathology associated with elevated levels of growth hormone and insulin-like growth factor I in transgenic mice. *Endocrinology*. 1989;124(1):40-48. doi:10.1210/endo-124-1-40
37. Doi T, Striker LJ, Gibson CC, Agodoa LY, Brinster RL, Striker GE. Glomerular lesions in mice transgenic for growth hormone and insulinlike growth factor-I. I. Relationship between increased glomerular size and mesangial sclerosis. *Am J Pathol*. 1990;137(3):541-552.
38. Franklin SC, Moulton M, Sicard GA, Hammerman MR, Miller SB. Insulin-like growth factor I preserves renal function postoperatively. *Am J Physiol*. 1997;272(2 Pt 2):F257-F259. doi:10.1152/ajprenal.1997.272.2.F257
39. Vijayan A, Franklin SC, Behrend T, Hammerman MR, Miller SB. Insulin-like growth factor I improves renal function in patients with end-stage chronic renal failure. *Am J Physiol*. 1999;276(4):R929-R934. doi:10.1152/ajpregu.1999.276.4.R929
40. Hammerman MR, Miller SB. Effects of growth hormone and insulin-like growth factor I on renal growth and function. *J Pediatr*. 1997;131(1 Pt 2):S17-S19. doi:10.1016/s0022-3476(97)70004-0
41. O'Shea MH, Miller SB, Hammerman MR. Effects of IGF-I on renal function in patients with chronic renal failure. *Am J Physiol*. 1993;264(5 Pt 2):F917-F922. doi:10.1152/ajprenal.1993.264.5.F917

SUPPLEMENTARY MATERIAL

Supplemental Figure 1.

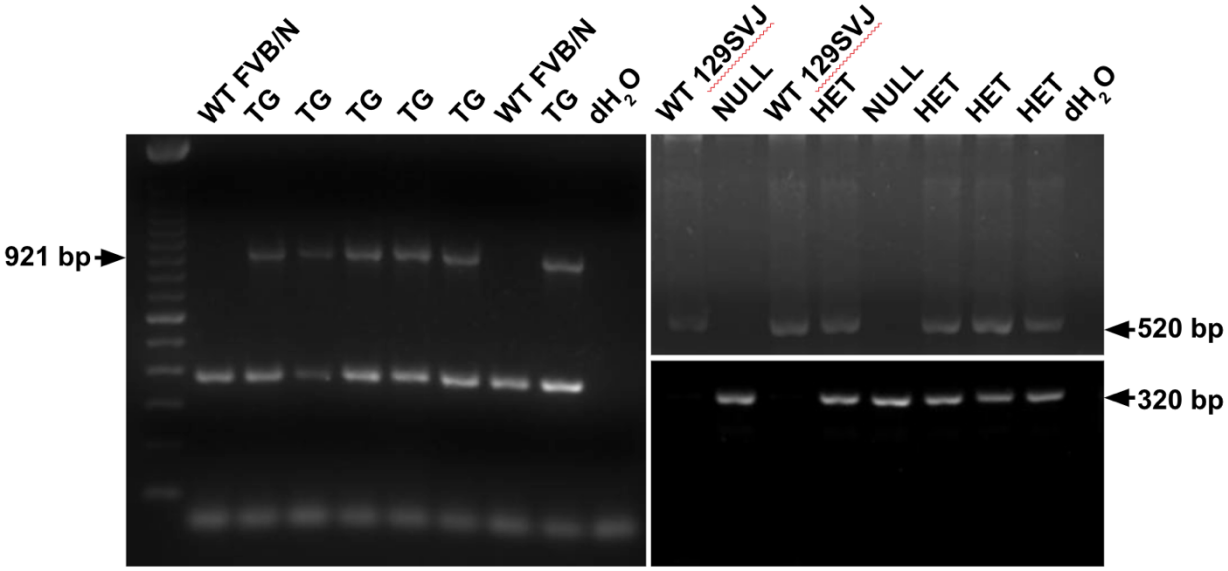

Supplemental Figure 1. DNA genotyping of HB-EGF TG, heterozygous, null, and wild-type strains of mice by polymerase chain reaction (PCR). The primers of human HB-EGF TG were used to amplify a 921 bp DNA product from HB-EGF TG mice. Genotyping HB-EGF null and heterozygous mice used a mouse HB-EGF wild type forward primer and a HB-EGF pSV-neo gene reverse primer and amplified a 320 bp DNA product in order to detect the null HB-EGF allele. The mouse HB-EGF wild type forward and reverse primers resulted in a 520 bp DNA product in wild type and heterozygous mice. Therefore, HB-EGF null mice are expected to result in a 320 bp DNA product only, HB-EGF wild type mice are expected to have a 520 bp DNA product only, while heterozygous mice are expected to have both 320 bp and 520 bp DNA products, and hHB-EGF TG mice are expected to have the 921bp transgene and an endogenous 320bp mHB-EGF product.

Supplemental Figure 2.

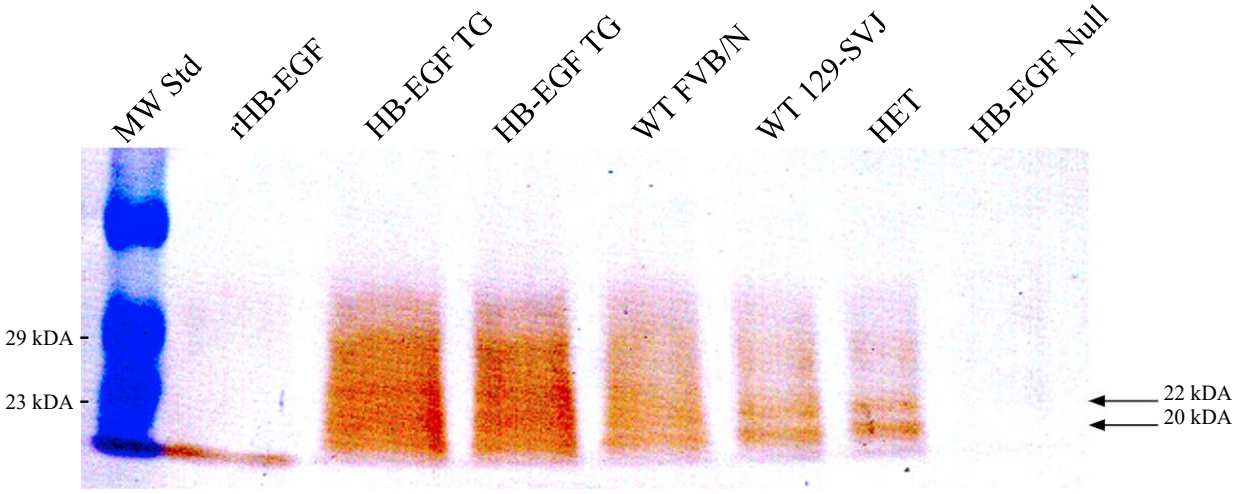

Supplemental Figure 2. HB-EGF immunoreactive proteins of 20-22kDA (indicated with arrows from total protein isolated from the kidney of HB-EGF TG, WT FVB/N and 129-SVJ, and heterozygous (HET), mice were detected with not HB-EGF immunoreactive proteins detected in HB-EGF Null mice. 1mg of recombinant HB-EGF standard (rHB-EGF) of kDa was used as a positive control.